JOURNAL OF MOLECULAR SPECTROSCOPY **186,** 113–130 (1997)
ARTICLE NO. MS977356

Fourier Transform Infrared Emission Spectroscopy of the $C^4\Delta$–$X^4\Phi$, $G^4\Phi$–$X^4\Phi$, and $G^4\Phi$–$C^4\Delta$ Systems of TiCl

R. S. Ram* and P. F. Bernath*,†

*Department of Chemistry, University of Arizona, Tucson, Arizona 85721; and †Department of Chemistry, University of Waterloo, Waterloo, Ontario, Canada N2L 3G1

Received May 2, 1997

The emission spectrum of TiCl has been investigated in the 3000–12 000 cm^{-1} region at high resolution using a Fourier transform spectrometer. The bands were excited in a microwave discharge through a flowing mixture of $TiCl_4$ and helium. The observed bands have been classified into three electronic transitions, $C^4\Delta$–$X^4\Phi$, $G^4\Phi$–$X^4\Phi$, and $G^4\Phi$–$C^4\Delta$. In the 3000–3500 cm^{-1} region, four bands with R heads at 3368.7, 3331.8, 3291.9, and 3243.4 cm^{-1} have been assigned as the 0–0 bands of the 1/2–3/2, 3/2–5/2, 5/2–7/2, and 7/2–9/2 subbands, respectively, of the $C^4\Delta$–$X^4\Phi$ transition. To higher wavenumbers, four transitions with 0–0 R heads at 10 930.7, 10 921.3, 10 906.5, and 10 886.9 cm^{-1} have been assigned as the 3/2–3/2, 5/2–5/2, 7/2–7/2, and 9/2–9/2 subbands, respectively, of the $G^4\Phi$–$X^4\Phi$ system of TiCl. Four additional bands with 0–0 R heads at 7568.8, 7596.4, 7622.2, and 7651.7 cm^{-1} have been identified as the 1/2–3/2, 3/2–5/2, 5/2–7/2, and 7/2–9/2 subbands of the $G^4\Phi$–$C^4\Delta$ transition, respectively. A rotational analysis of a number of vibrational bands of these transitions has been obtained and molecular constants have been extracted. The lowest $^4\Phi$ state has been assigned as the ground state of TiCl, by analogy with our recent work on TiF (R. S. Ram and P. F. Bernath, *J. Mol. Spectrosc.*, in press). The correspondence between the electronic states of TiCl, TiF, TiH, and Ti^+ is also discussed.

INTRODUCTION

The atomic lines of transition metal elements are prominent in stellar spectra (*1*). The presence of several transition metal oxides (*1–8*) and hydrides (*9–13*) is also well established in cool stars, particularly in S- and M-type stars and in sunspots. So far no transition metal halides have been identified in stellar spectra, partly because of a lack of laboratory data. The observation of metal halides such as NaCl, KCl, AlCl, and AlF in the atmosphere of the carbon star IRC +10216 by millimeter-wave astronomers (*14, 15*) strengthens the possibility that transition metal chloride and fluoride molecules will be found. These observations are partly responsible for a renewed interest in the spectroscopy of transition metal halides (*16, 17*). In some cases such as for TiCl, even the identity of the ground electronic state has been in question. The reason for this state of affairs is the complexity of the visible spectra of transition metal halides. The presence of open *d* shells in transition metal elements often results in a high density of close-lying electronic states with high multiplicity and large orbital angular momenta. The numerous close-lying electronic states perturb each other extensively. TiCl is typical in that complex spectra have been known for nearly a century, but a definitive assignment of the ground state and the low-lying electronic states has yet to be carried out.

The electronic spectrum of TiCl was first observed in 1907 by Fowler (*18*) who observed complex banded structure in the 400–420 nm region using an arc source. This work was followed by several attempts (*19–25*) to obtain a vibrational classification of these bands using the spectra recorded in emission as well as in absorption. More and Parker (*19*) assigned the strong bands in this region to a doublet transition, while Rao (*20*) assigned the same bands to a $^4\Pi$–$^4\Sigma^-$ transition. The analysis of Rao (*20*) was criticized by Shenyavskaya *et al.* (*21*) who proposed new assignments for the same bands, although they retained the $^4\Pi$–$^4\Sigma^-$ electronic assignment. Similar assignments were also proposed by Chatalic *et al.* (*22*) and Diebner and Kay (*23*). These analyses were later disputed by Lanini (*24*) who obtained a rotational analysis of a few strong bands and assigned them to a $^2\Phi$–$^2\Delta$ transition. More recently a rotational analysis of a number of bands in the 409.5–420 nm region was obtained by Phillips and Davis (*26*) who classified these bands into four doublet electronic transitions.

Recently we observed a $^4\Phi$–$^4\Phi$ transition of TiF by Fourier transform emission spectroscopy and by laser excitation spectroscopy (*27*). The ground state of TiF was identified as the $X^4\Phi$ state. This assignment was supported by a recent ab initio calculation of Harrison (*28*) who predicted the spectroscopic properties of the ground state and a number of low-lying excited electronic states. Our assignment was also consistent with expectations based on available results for isovalent TiH (*29–32*). The electronic structure of TiCl

0022-2852/97 $25.00

should be very similar to that of TiF so that we also expect a $^4\Phi$ ground state for TiCl. The other low-lying electronic states will be $^4\Sigma^-$, $^4\Pi$, and $^4\Delta$ in the quartet manifold and $^2\Phi$, $^2\Delta$, $^2\Pi$, and $^2\Sigma^-$ states in the doublet manifold, as predicted for TiF (*28*) and TiH (*29*).

In the present paper we report on the observation of three new electronic transitions of TiCl, $C^4\Delta$–$X^4\Phi$, $G^4\Phi$–$X^4\Phi$, and $G^4\Phi$–$C^4\Delta$, in the 3000–12 000 cm^{-1} region with the $X^4\Phi$ state assigned as the ground state. We base the letter notation for these states on the recent theoretical predictions of Harrison (*28*) for TiF and the data available for TiH (*29–32*). The rotational analysis of these band systems provides the first high-resolution spectroscopic data for all four spin components of the ground state of TiCl. Several weaker bands and a few strong complex bands remain to be analyzed in the 3000–12 000 cm^{-1} interval.

EXPERIMENTAL DETAILS

The emission spectra of TiCl were produced in an electrodeless microwave discharge through a flowing mixture of 30 mTorr of $TiCl_4$ vapor and 3 Torr of He. The discharge tube was made of quartz and had an outer diameter of 12 mm. The liquid $TiCl_4$ sample was placed in a small bulb at room temperature and the partial pressure of $TiCl_4$ in the discharge tube was regulated with a needle valve. The TiCl bands appeared strongly when the discharge had an intense blue–white color. The emission from the discharge tube passed directly through the 8-mm entrance aperture of the 1-m Fourier transform spectrometer of the National Solar Observatory at Kitt Peak. The spectra in the 1800–9000 cm^{-1} interval were recorded using liquid nitrogen cooled InSb detectors and Si filters. A total of 11 scans were co-added in about 80 min of integration at a resolution of 0.02 cm^{-1}. The 9000–12 500 cm^{-1} range was recorded with Si photo diode detectors and a red pass filter (RG 850) but the CaF_2 beam splitter had poor efficiency above 9000 cm^{-1}.

The spectral line positions were determined using a data reduction program called PC-DECOMP developed by J. Brault. The peak positions were determined by fitting a Voigt lineshape function to each line. The spectra were calibrated using the wavenumbers of the vibration–rotation lines of the 1–0 band of HCl (*33*) which appeared in emission in the same spectrum. There was enough overlap between the two spectral regions to bring them to the same wavenumber scale. The molecular lines of TiCl have a typical width of 0.03 cm^{-1} and appear with a maximum signal-to-noise ratio of 20:1 so that the best line positions are expected to be accurate to about ± 0.002 cm^{-1}.

DESCRIPTION OF OBSERVED BANDS

The spectrum of TiCl contains a large number of bands spread over the 3000–12 000 cm^{-1} region. After rotational analysis of a number of strong bands, it became clear that there were three transitions with 0–0 bands located in the 3000–3400, 10 500–11 000, and 7500–7560 cm^{-1} intervals, assigned as the $C^4\Delta$–$X^4\Phi$, $G^4\Phi$–$X^4\Phi$, and $G^4\Phi$–$C^4\Delta$ transitions, respectively, of TiCl. The lines in different bands were sorted into branches using a color Loomis–Wood program running on a PC computer.

A correlation diagram of the energy levels of TiCl, TiF, TiH, and Ti^+ is presented in Fig. 1. Although no theoretical calculations are available for TiCl, energy levels are drawn on the basis of available data for the isovalent molecule TiF (*28*). The ground state of TiF has been assigned as $X^4\Phi$ from experimental observations (*27*) and theoretical calculations (*28*). TiF has a number of low-lying electronic states with quartet and doublet multiplicity. In the quartet manifold of states, the $^4\Sigma^-$ state is predicted to be 0.1 eV above the ground state. A $^4\Phi$ state of TiF at 15 033 cm^{-1} was assigned as the $G^4\Phi$ state (Fig. 1). A comparison of the observed positions of the new electronic states of TiCl and TiF leads to the labeling of the $^4\Phi$ state of TiCl at 10 900 cm^{-1} as the $G^4\Phi$ state. The $C^4\Delta$ state of TiF has yet to be identified. In addition to the transitions analyzed in this work, several additional bands remain to be assigned. Some of these bands are weaker in intensity while the other strong bands have a very complex structure. In particular the bands centered at 5150 and 6600 cm^{-1} seem to have several subbands overlapped in a narrow wavenumber range. Improved spectra at higher resolution are required to analyze these bands.

As predicted by Harrison (*28*) for TiF, there should also be a number of low-lying doublet electronic states for TiCl. Some of the weaker unassigned bands may involve doublet–doublet transitions. We have just recorded additional spectra in the 10 000–25 000 cm^{-1} region, in order to identify other low-lying electronic states of TiCl. In this paper we report on the rotational analysis of the bands of the $C^4\Delta$–$X^4\Phi$, $G^4\Phi$–$X^4\Phi$, and $G^4\Phi$–$C^4\Delta$ transitions (Fig. 2). We have determined the molecular constants only for the most abundant $^{48}Ti^{35}Cl$ isotopomer. Some weak lines of the $^{48}Ti^{37}Cl$ isotopomer have also been observed in the strong bands but the data were not sufficient for rotational analysis. The lines involving the less abundant ^{46}Ti (8%), ^{47}Ti (7.3%), ^{49}Ti (5.5%), and ^{50}Ti (5.4%) isotopes were not identified because of their weak intensity.

1. *The $C^4\Delta$–$X^4\Phi$ Transition*

The four red degraded bands with *R* heads at 3368.5, 3331.8, 3292.0, and 3243.5 cm^{-1} have been assigned as the 0–0 bands of the $^4\Delta_{1/2}$–$^4\Phi_{3/2}$, $^4\Delta_{3/2}$–$^4\Phi_{5/2}$, $^4\Phi_{5/2}$–$^4\Phi_{7/2}$, and $^4\Delta_{7/2}$–$^4\Phi_{9/2}$ subbands, respectively. A compressed part of the spectrum of this transition is presented in Fig. 3. The 0–0 bands are followed by weak 1–1 bands with *R* heads at 3341.6, 3304.1, 3263.1, and 3216.3 cm^{-1}, respectively.

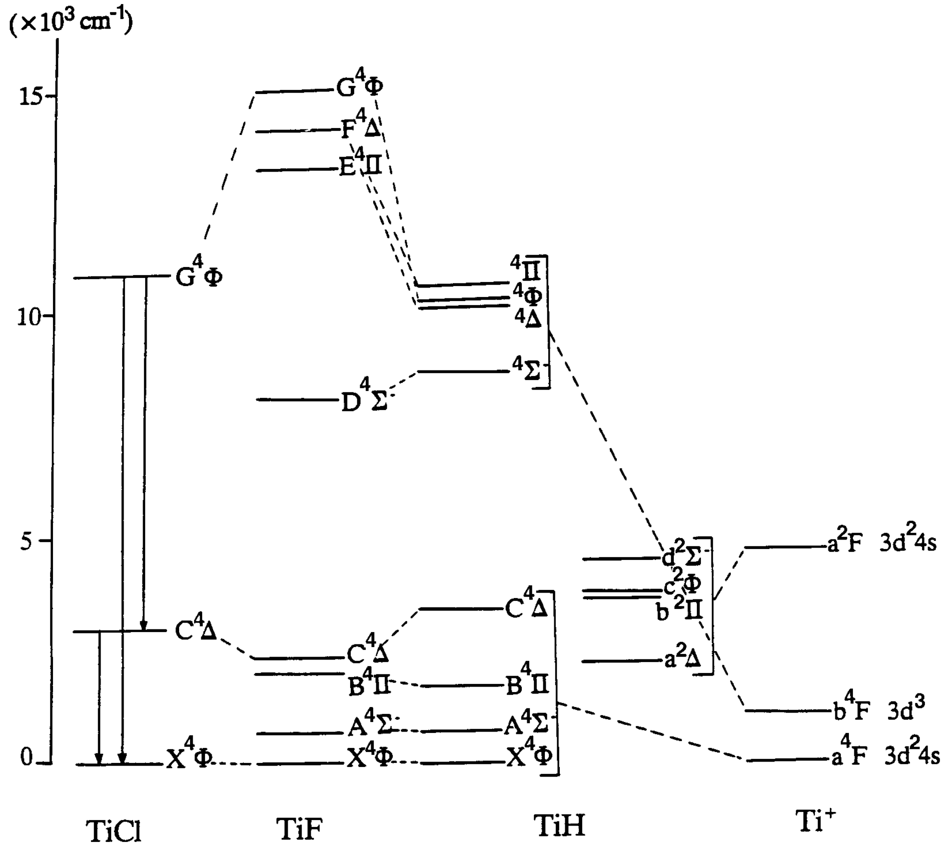

FIG. 1. A correlation diagram of the electronic energy levels of TiCl, TiF (*28*), and TiH (*29*) with the atomic energy levels of Ti^+ (*37*). The energy levels of TiH are taken from ab initio calculation (*29*) while those for TiF are based on ab initio calculation (*28*) and partly on our empirical estimates. The observed TiCl transitions are marked with arrows.

Rotational analysis of the 1–1 band was not attempted because of weak intensity. Off-diagonal bands with $\Delta v \neq 0$ were not seen in our spectra.

The structure of each of the subbands consists of single P, Q, and R branches, without any Ω doubling. A perturbation has been observed in the $v = 0$ vibrational level of the $C^4\Delta_{3/2}$ spin component at $J' \geqslant 29.5$, and perturbed lines could not be identified. An expanded portion of the 1/2–3/2 subband is presented in Fig. 4.

2. *The $G^4\Phi$–$X^4\Phi$ Transition*

In the 10 000–12 000 cm^{-1} region, five groups of bands with the highest wavenumber R heads at 10 125, 10 527, 10 931, 11 276, and 11 619 cm^{-1} have been assigned as the 0–2, 0–1, 0–0, 1–0, and 2–0 bands of the $G^4\Phi$–$X^4\Phi$ transition. A closer inspection of these bands indicates that each vibrational band consists of four subbands as expected for a $^4\Phi$–$^4\Phi$ transition. In the 0–0 band, for example, the four subbands with R heads at 10 931, 10 921, 10 907, and 10 887 cm^{-1} have been identified as the $^4\Phi_{9/2}$–$^4\Phi_{9/2}$, $^4\Phi_{7/2}$–$^4\Phi_{7/2}$, $^4\Phi_{5/2}$–$^4\Phi_{5/2}$, and $^4\Phi_{3/2}$–$^4\Phi_{3/2}$ subbands (Fig. 5). Each of these subbands consists of single R and single P branches as expected for a $\Delta\Omega = 0$ transition with no Ω doubling. The rotational analysis of the bands of this transition indicates that the lower state is in common with the previously analyzed $C^4\Delta$–$X^4\Phi$ transition.

We have obtained the rotational analysis of the 0–1, 0–0, and 1–0 bands of the $G^4\Phi$–$X^4\Phi$ transition. Although the 2–0 band is prominent in the spectra, strong perturbations in the excited state make the structure relatively complex. For this reason, no analysis of the 2–0 band was attempted at this time. The analysis of other bands such as 0–2, 1–2, 1–1, or 2–1 was not attempted because of their weak intensity. Several local perturbations have been observed in the $G^4\Phi$ state. A local perturbation has been found in the $v = 0$ vibrational level of the $G^4\Phi_{3/2}$ spin component near $J = 19.5$. The $v = 1$ vibrational level of the $G^4\Phi$ state is also perturbed in the $G^4\Phi_{3/2}$ ($J > 52.5$), $G^4\Phi_{5/2}$ ($J > 33.5$), and $G^4\Phi_{7/2}$ ($J > 43.5$) spin components. In some bands the perturbed lines as well as those with J values higher than the J value of a strong perturbation could not be identified.

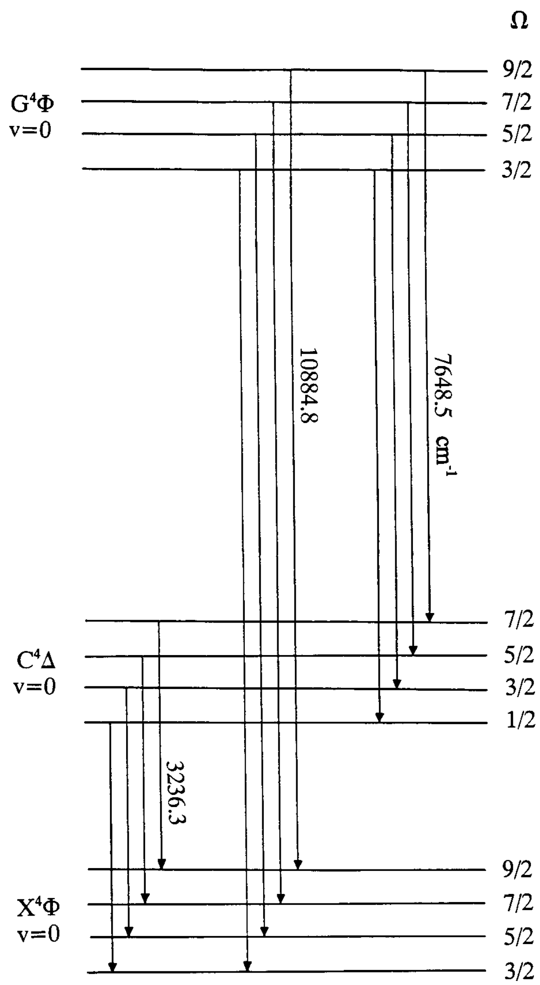

FIG. 2. A schematic energy level diagram of the observed transitions of TiCl. The band origins for subbands involving the highest spin component of each state are also listed.

A portion of the high-resolution spectrum of the 3/2–3/2 subband of the 0–0 band is presented in Fig. 6.

3. The $G^4\Phi$–$C^4\Delta$ Transition

Another group of four subbands was identified in the 7500–7650 cm^{-1} interval. These subbands have been assigned as the transition between the two excited states of the $C^4\Delta$–$X^4\Phi$ and $G^4\Phi$–$X^4\Phi$ transitions. The $G^4\Phi$–$C^4\Delta$ transition of TiCl has four subbands with R heads at 7586.8, 7696.4, 7622.2, and 7651.7 cm^{-1} assigned as $^4\Phi_{3/2}$–$^4\Delta_{1/2}$, $^4\Phi_{5/2}$–$^4\Delta_{3/2}$, $^4\Phi_{7/2}$–$^4\Delta_{5/2}$, and $^4\Phi_{9/2}$–$^4\Delta_{7/2}$, respectively. The analysis of this transition confirms the analysis of the $C^4\Delta$–$X^4\Phi$ and $G^4\Phi$–$X^4\Phi$ transitions. A compressed portion of the 0–0 band of the $G^4\Phi$–$C^4\Delta$ transition is presented in Fig. 7. Only the 0–0 band could be identified in our spectra. Each subband consists of single P, Q, and R branches, as

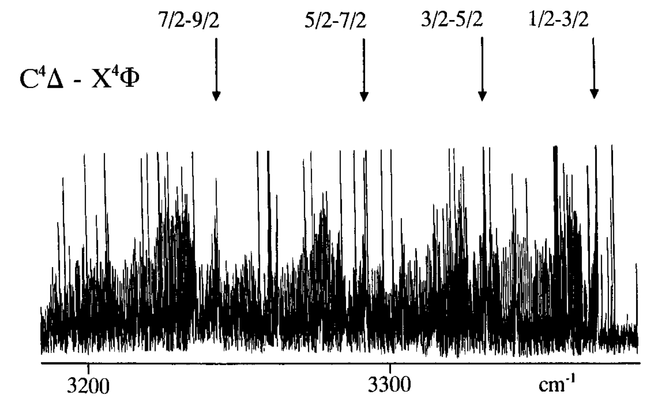

FIG. 3. A compressed portion of the 0–0 band of the $C^4\Delta$–$X^4\Phi$ transition of TiCl with the subband R heads marked with arrows.

expected. The rotational perturbations observed in the $C^4\Delta$ and $G^4\Phi$ states have also been confirmed from the analysis of this transition. An expanded portion of the 9/2–7/2 subbands near the R head is presented in Fig. 8.

ANALYSIS AND RESULTS

Since each of the three observed transitions has at least one state in common, the rotational assignments in the different bands were made by comparing combination differences for the common vibrational levels. As is often the case, no transitions having $\Delta\Sigma \neq 0$ were observed and the spin–orbit intervals could not be determined directly. The subbands of different spin components were initially fitted separately using a simple term energy expression (Eq. [1]), although the observed $^4\Phi$ electronic states most likely obey Hund's case (a) coupling.

$$F_v(J) = T_v + B_vJ(J+1) - D_v[J(J+1)]^2 + H_v[J(J+1)]^3 \quad [1]$$

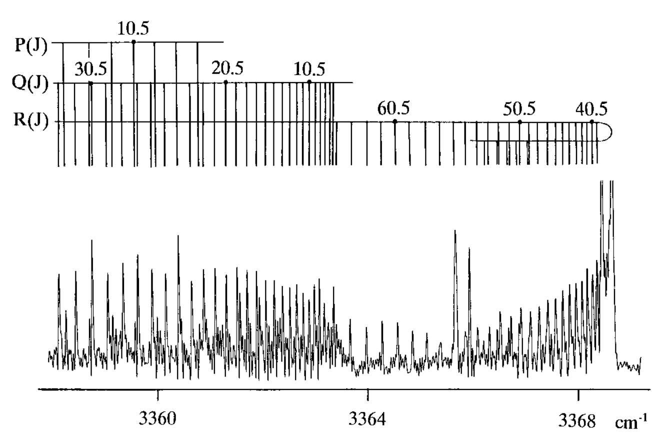

FIG. 4. An expanded portion of the $C^4\Delta_{1/2}$–$X^4\Phi_{3/2}$ subband of TiCl near the R head.

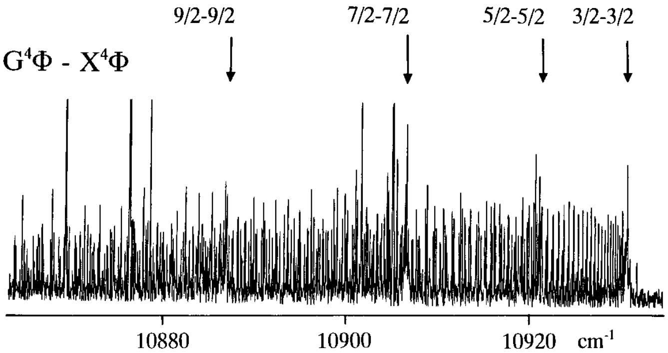

FIG. 5. A compressed portion of the 0–0 band of the $G^4\Phi$–$X^4\Phi$ transition of TiCl with the subband *R* heads marked with arrows.

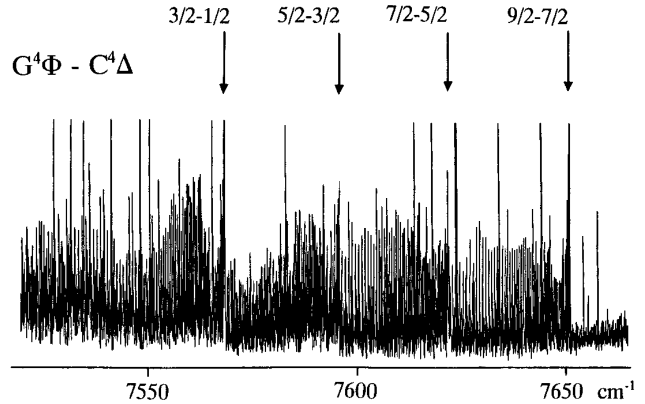

FIG. 7. A compressed portion of the 0–0 band of the $G^4\Phi$–$C^4\Delta$ transition of TiCl with the subband *R* heads marked with arrows.

This initial band-by-band fit of different bands provided similar constants for common vibrational levels, confirming the vibrational and rotational assignments. In the final fit, the lines of all of the vibrational bands in each subband were combined and fitted simultaneously. The observed lines positions for the $C^4\Delta$–$X^4\Phi$ and $G^4\Phi$–$C^4\Delta$ transitions are provided in Table 1 and the line positions for the $G^4\Phi$–$X^4\Phi$ transition are provided in Table 2.

The rotational lines were weighted according to resolution, extent of blending, and effect of perturbations. Perturbed lines were not included in the fit and the badly blended lines were heavily deweighted. The higher order effective constant H_v is also required in some spin components of the $C^4\Delta$ and $G^4\Phi$ states because of global interactions in the excited states. The molecular constants for the $X^4\Phi$, $C^4\Delta$, and $G^4\Phi$ states obtained from these fits are provided in Tables 3, 4, and 5, respectively.

DISCUSSION

Although no theoretical calculations are available for TiCl, a recent ab initio calculation for TiF (*28*) may be used as a guide since the electronic states of TiCl and TiF are expected to be very similar. In fact the observed $X^4\Phi$, $C^4\Delta$, and $G^4\Phi$ states are nicely consistent with expectations based on previous TiF work (*27*). Also, the ordering of low-lying electronic states of transition metal fluorides and hydrides is very similar. These similarities have been noted by us and other workers and a detailed comparison for the CoH/CoF (*34*), FeH/FeF (*35*), ScH/ScF (*36*), and TiF/TiH (*27*) pairs has been reported previously. As discussed in our paper on TiF (*27*), the low-lying electronic states of TiF correlate directly to the states of Ti^+ as do the electronic states of TiH (*29*). The observed electronic states of TiCl also seem to follow a similar pattern suggesting that the electronic states of TiCl, TiF, TiH, and Ti^+ are all similar.

The Cl^-, F^-, and H^- ligands give rise to similar energy level patterns in TiCl, TiF, and TiH, although the bonding in TiH is expected to be much more covalent than in TiCl and TiF. A correlation diagram of the low-lying electronic states of TiCl, TiF, TiH, and Ti^+ is provided in Fig. 1. As

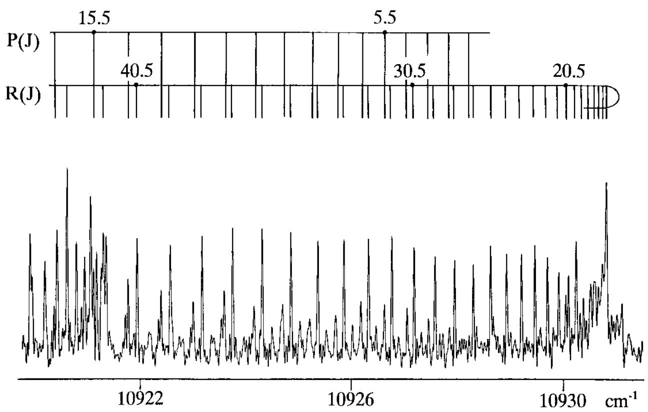

FIG. 6. An expanded portion of the $G^4\Phi_{3/2}$–$X^4\Phi_{3/2}$ subband of TiCl near the *R* head.

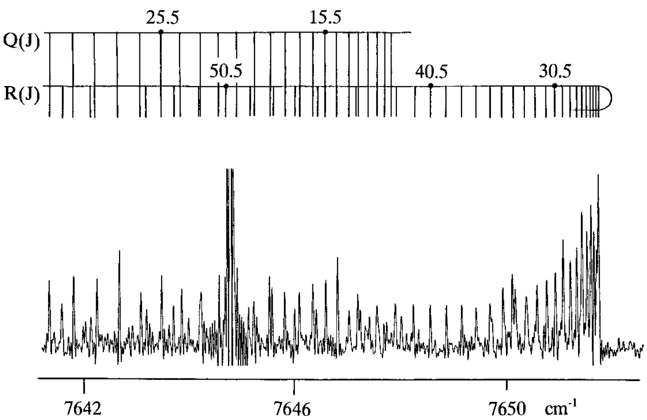

FIG. 8. An expanded portion of the $G^4\Phi_{9/2}$–$C^4\Delta_{7/2}$ subband of TiCl near the *R* head.

TABLE 1
Observed Line Positions (in cm^{-1}) for the $C^4\Delta - X^4\Phi$ and $G^4\Phi - C^4\Delta$ Transitions of TiCl

	$C^4\Delta_{1/2}$ - $X^4\Phi_{3/2}$ 0 - 0						$G^4\Phi_{3/2}$ - $C^4\Delta_{1/2}$ 0 - 0					
J	R(J)	O-C	P(J)	O-C	Q(J)	O-C	R(J)	O-C	P(J)	O-C	Q(J)	O-C
2.5					3363.454	9						
3.5					3363.412	1						
4.5			3361.959	2	3363.360	-6						
5.5			3361.590	0	3363.312	0					7564.970	2
6.5	3365.601	2	3361.212	-1	3363.253	3					7564.881	-2
7.5	3365.841	3	3360.824	-4	3363.183	7					7564.787	2
8.5	3366.076	8	3360.437	6	3363.093	0					7564.677	2
9.5	3366.298	10	3360.026	1	3363.000	-1	7567.699	-4	7561.70	1	7564.559	8
10.5	3366.505	6	3359.608	-2	3362.898	0	7567.859	-7	7561.27	2	7564.418	3
11.5	3366.710	10	3359.186	2	3362.787	2	7568.013	-3			7564.275	10
12.5	3366.899	8	3358.749	-1	3362.668	4	7568.154	0	7560.35	-3	7564.107	4
13.5	3367.080	8	3358.306	1	3362.532	0	7568.272	-7	7559.88	2	7563.932	5
14.5	3367.248	5	3357.853	2	3362.393	3	7568.387	-2	7559.39	4	7563.743	5
15.5	3367.414	8	3357.388	2	3362.238	-1	7568.491	3	7558.90	13	7563.546	10
16.5	3367.557	0	3356.913	1	3362.078	0	7568.579	6*	7558.38	10	7563.336	14
17.5	3367.700	1	3356.438	9	3361.907	-1			7557.86	16*	7563.112	18*
18.5	3367.831	0	3355.931	-4	3361.727	0	7568.789	86*	7557.32	21*	7562.877	24*
19.5	3367.952	-2			3361.535	-2	7568.714	-35*			7562.681	81*
20.5	3368.066	-1			3361.336	-1			7556.27	90*	7562.303	-29*
21.5	3368.164	-6	3354.394	-3	3361.126	-1	7568.789	-12	7555.58	-25*	7562.037	-15*
22.5	3368.265	3	3353.865	0	3360.907	0	7568.789	-18	7554.99	-14*	7561.750	-9
23.5	3368.349	3	3353.322	-1	3360.681	2	7568.789	-11	7554.40	-8	7561.444	-9
24.5	3368.409	-11	3352.782	9	3360.437	-3	7568.789	9	7553.77	-10	7561.125	-8
25.5			3352.197	-14	3360.192	1	7568.743	-5	7553.14	-10	7560.796	-4
26.5			3351.635	-5	3359.932	-1	7568.707	7	7552.51	-1	7560.451	-4
27.5			3351.059	-1	3359.666	1	7568.652	11	7551.85	0	7560.092	-4
28.5			3350.473	3	3359.387	0	7568.579	10	7551.17	-7	7559.722	-2
29.5			3349.872	2	3359.097	-3	7568.491	8	7550.49	-2	7559.336	-4
30.5			3349.250	-11	3358.804	2	7568.387	4	7549.80	1	7558.934	-7
31.5			3348.651	9	3358.495	-1	7568.272	1	7549.09	-1	7558.527	-2
32.5			3348.017	3	3358.175	-4	7568.154	10	7548.37	7	7558.111	5
33.5			3347.375	0	3357.853	0	7568.013	8	7547.63	2	7557.673	6
34.5			3346.724	-3	3357.519	3	7567.859	6	7546.88	0	7557.218	2
35.5			3346.069	-1	3357.173	2	7567.699	12	7546.12	2	7556.755	3
36.5			3345.398	-5	3356.817	1	7567.509	1	7545.34	1	7556.279	4
37.5			3344.725	-1	3356.438	-12	7567.326	10			7555.782	-2
38.5	3368.409	-14	3344.037	-3	3356.072	-3	7567.122	12	7543.75	-3	7555.276	-4
39.5	3368.349	-1	3343.342	-2			7566.902	11	7542.92	-17	7554.762	-1
40.5	3368.265	-1	3342.632	-7			7566.670	12	7542.09	-10	7554.224	-8
41.5	3368.164	-10	3341.916	-7			7566.411	-2	7541.27	11	7553.689	0
42.5	3368.066	-6	3341.192	-7	3354.470	-10	7566.153	0	7540.41	4	7553.143	11
43.5	3367.952	-7	3340.445	-20	3354.051	-6	7565.876	-5	7539.55	13	7552.569	8
44.5	3367.831	-7	3339.730	8	3353.629	5	7565.587	-7	7538.67	7	7551.989	11
45.5	3367.700	-6	3338.955	-13	3353.191	9	7565.296	1			7551.392	12
46.5	3367.557	-8	3338.209	4	3352.740	10			7536.85	-9	7550.769	-1
47.5	3367.414	0	3337.438	4	3352.278	10	7564.668	14	7535.94	10	7550.143	-3
48.5	3367.248	-4	3336.662	11	3351.805	9	7564.317	3	7535.00	-4	7549.514	5
49.5	3367.080	-2	3335.863	3	3351.322	6	7563.962	2	7534.06	6		
50.5	3366.899	-3	3335.070	10	3350.830	5	7563.590	-2	7533.09	-6	7548.186	-8
51.5	3366.710	-2	3334.260	11	3350.331	6	7563.206	-6	7532.11	-6	7547.511	-6
52.5	3366.505	-7	3333.435	5	3349.819	4	7562.816	-1			7546.824	-1
53.5	3366.298	-4	3332.603	3	3349.299	3	7562.399	-9	7530.13	5	7546.118	-3
54.5	3366.076	-6	3331.743	-18	3348.770	3	7561.984	-2	7529.12	1	7545.401	-1
55.5	3365.841	-13	3330.899	-15	3348.232	3	7561.549	-2			7544.669	-2
56.5	3365.601	-15	3330.060	4	3347.684	3			7527.04	-6	7543.921	-5
57.5	3365.365	-2	3329.196	8	3347.123	0	7560.646	8	7525.98	-8	7543.170	3
58.5	3365.114	5	3328.311	-1	3346.567	11	7560.151	-11	7524.93	4	7542.383	-12
59.5	3364.844	3			3345.985	6	7559.660	-11	7523.83	-11	7541.604	-5
60.5	3364.564	1	3326.537	6	3345.398	5	7559.158	-8	7522.75	4	7540.801	-8
61.5	3364.275	-1	3325.633	7	3344.800	3	7558.648	-1	7521.64	5	7539.987	-9
62.5	3363.978	-1	3324.718	5	3344.191	0	7558.111	-6	7520.52	2	7539.170	1
63.5	3363.671	-1	3323.790	2	3343.574	-2	7557.569	-1			7538.325	-4
64.5	3363.360	4	3322.852	-4	3342.949	-3	7557.019	8	7518.23	-4	7537.475	1
65.5	3363.040	9	3321.906	-8	3342.315	-3	7556.437	0	7517.08	8	7536.612	6
66.5			3320.956	-6	3341.670	-4			7515.90	9	7535.733	8
67.5	3362.340	-10			3341.017	-4			7514.71	5	7534.833	4

Note: O-C are observed minus calculated line positions in units of 10^{-3} cm^{-1} and asterisks mark perturbed lines.

TABLE 1—*Continued*

	$C^4\Delta_{1/2}$ - $X^4\Phi_{3/2}$						$G^4\Phi_{3/2}$ - $C^4\Delta_{1/2}$					
	0 - 0						0 - 0					
J	R(J)	O-C	P(J)	O-C	Q(J)	O-C	R(J)	O-C	P(J)	O-C	Q(J)	O-C
68.5	3362.001	6			3340.352	-6					7533.921	2
69.5	3361.630	0			3339.687	0			7512.29	3	7533.000	4
70.5	3361.258	2			3338.998	-8			7511.06	3	7532.067	8
71.5					3338.309	-6			7509.81	6	7531.114	6
72.5	3360.478	-1			3337.611	-3			7508.55	-2	7530.142	0
73.5	3360.077	2			3336.900	-4			7507.28	4	7529.167	3
74.5	3359.666	3			3336.183	-2			7505.99	2	7528.163	-7
75.5	3359.241	1			3335.452	-4			7504.69	-8	7527.169	5
76.5	3358.804	-4			3334.720	2					7526.141	-2
77.5											7525.108	1
78.5											7524.063	4
79.5											7522.993	-3
80.5											7521.916	-2
81.5											7520.817	-10

	$C^4\Delta_{3/2}$ - $X^4\Phi_{5/2}$						$G^4\Phi_{5/2}$ - $C^4\Delta_{3/2}$					
	0 - 0						0 - 0					
J	R(J)	O-C	P(J)	O-C	Q(J)	O-C	R(J)	O-C	P(J)	O-C	Q(J)	O-C
6.5											7592.788	-17
7.5					3325.841	6					7592.696	-1
8.5					3325.760	-1					7592.573	-1
9.5					3325.674	-6			7589.58	5	7592.439	3
10.5			3322.281	1	3325.583	-7	7595.741	0	7589.14	15	7592.292	9
11.5			3321.862	-5	3325.481	-9	7595.879	4	7588.65	-10	7592.116	-1
12.5	3329.636	-2	3321.450	6	3325.380	-3	7595.988	-6	7588.17	-8	7591.936	0
13.5	3329.840	4	3321.017	4	3325.278	11	7596.094	-5	7587.68	-3	7591.742	2
14.5			3320.575	3	3325.140	-2	7596.184	-5			7591.530	0
15.5	3330.204	-4	3320.136	11	3325.006	-3	7596.256	-8	7586.64	-7	7591.304	0
16.5	3330.378	-4	3319.669	1	3324.864	-4	7596.324	-1	7586.10	-2	7591.064	-1
17.5	3330.548	0	3319.204	1	3324.718	0	7596.373	3	7585.54	-8	7590.810	0
18.5	3330.706	1	3318.728	-2	3324.561	1	7596.411	10	7584.99	13	7590.541	0
19.5	3330.859	5	3318.245	-3	3324.390	-3	7596.411	-6	7584.40	0	7590.257	1
20.5	3331.002	6	3317.763	4	3324.220	0	7596.411	-6	7583.82	24	7589.958	2
21.5	3331.131	2	3317.260	-1	3324.041	4	7596.411	9	7583.18	5	7589.643	2
22.5			3316.754	-2	3323.846	-2	7596.373	3	7582.54	-9	7589.310	0
23.5			3316.249	6	3323.652	1	7596.324	1	7581.90	-3	7588.967	5
24.5			3315.726	2	3323.455	6	7596.256	-3	7581.24	1	7588.599	1
25.5	3331.595	-1	3315.202	5	3323.240	2	7596.184	6	7580.55	-5	7588.223	5
26.5	3331.696	-1	3314.664	-1	3323.019	-3	7596.094	13	7579.87	10	7587.825	4
27.5	3331.786	-8	3314.118	-7			7595.988	22	7579.14	-3	7587.404	-2
28.5			3313.580	-1					7578.41	0	7586.968	-4
29.5			3313.037	5					7577.65	-15	7586.502	-18

	$C^4\Delta_{5/2}$ - $X^4\Phi_{7/2}$						$G^4\Phi_{7/2}$ - $C^4\Delta_{5/2}$					
	0 - 0						0 - 0					
J	R(J)	O-C	P(J)	O-C	Q(J)	O-C	R(J)	O-C	P(J)	O-C	Q(J)	O-C
3.5					3285.375	21	7620.228	-3				
4.5					3285.327	9	7620.466	0				
5.5					3285.280	5	7620.665	-22				
6.5			3283.522	-11	3285.231	7	7620.900	8			7618.619	-8
7.5			3283.162	-3	3285.161	-5	7621.070	-11			7618.512	-3
8.5			3282.769	-20	3285.105	6	7621.256	-1			7618.384	-4
9.5	3288.354	3	3282.410	4	3285.019	-5	7621.413	-4			7618.251	4
10.5			3282.024	9	3284.942	0	7621.564	2	7614.91	-6	7618.084	-5
11.5			3281.609	-6	3284.857	5	7621.689	-3	7614.45	8	7617.913	-5
12.5	3289.037	6	3281.211	3	3284.754	0	7621.808	1			7617.732	0
13.5	3289.244	3	3280.798	4	3284.643	-5	7621.899	-9	7613.46	4	7617.527	-3
14.5	3289.432	-13	3280.366	-6	3284.535	1	7621.995	3	7612.93	-2	7617.313	-1
15.5	3289.617	-22	3279.945	4	3284.411	-2			7612.40	-3	7617.081	-1
16.5	3289.818	-9	3279.496	-7					7611.86	1	7616.842	6
17.5	3290.006	-1	3279.058	1					7611.29	-3	7616.576	2

TABLE 1—*Continued*

	$C^4\Delta_{5/2}$ - $X^4\Phi_{7/2}$						$G^4\Phi_{7/2}$ - $C^4\Delta_{5/2}$					
	0 - 0						0 - 0					
J	R(J)	O-C	P(J)	O-C	Q(J)	O-C	R(J)	O-C	P(J)	O-C	Q(J)	O-C
18.5	3290.172	-6	3278.608	4	3284.003	1			7610.71	-1	7616.297	-1
19.5	3290.342	0	3278.140	-3	3283.851	2			7610.13	5	7616.006	-1
20.5	3290.495	-3	3277.675	2	3283.689	0			7609.52	1	7615.704	4
21.5	3290.651	5	3277.217	20	3283.522	1	7622.187	19	7608.90	10	7615.377	-2
22.5	3290.783	-4	3276.704	-8	3283.344	-1	7622.143	10	7608.26	4	7615.044	1
23.5	3290.922	3			3283.162	1	7622.080	-3	7607.60	-6	7614.692	0
24.5	3291.047	3	3275.714	-5	3282.967	-2	7622.007	-10	7606.94	2	7614.326	1
25.5	3291.158	-3	3275.206	-6	3282.769	-2	7621.944	8	7606.25	1	7613.946	3
26.5	3291.265	-5	3274.713	17	3282.562	-1	7621.855	14	7605.54	-16	7613.551	4
27.5	3291.372	0	3274.172	-2	3282.349	-1	7621.733	3	7604.83	-6	7613.141	6
28.5	3291.460	-6			3282.127	0	7621.601	-3	7604.11	-1	7612.710	2
29.5	3291.531	-21	3273.104	0	3281.898	1	7621.468	5	7603.37	0	7612.267	2
30.5	3291.633	2	3272.565	6	3281.659	-1	7621.306	1	7602.61	1	7611.809	2
31.5	3291.701	0	3272.003	-2	3281.417	2	7621.134	0	7601.84	-2	7611.335	0
32.5			3271.443	-1	3281.165	3	7620.946	0	7601.05	-1	7610.848	1
33.5			3270.881	5	3280.902	0	7620.745	3	7600.24	-3	7610.348	5
34.5			3270.301	1	3280.637	2	7620.527	3	7599.43	2	7609.822	-3
35.5			3269.712	-5	3280.366	6	7620.287	-3	7598.59	-4	7609.290	0
36.5			3269.131	5	3280.077	-1	7620.049	9	7597.74	-3	7608.739	-1
37.5			3268.528	0	3279.786	-3	7619.779	4	7596.87	-2	7608.174	-1
38.5			3267.921	-2	3279.496	4	7619.496	2	7595.99	-6	7607.595	1
39.5			3267.316	5	3279.186	-2	7619.192	-6	7595.11	13	7606.996	-2
40.5			3266.690	-1	3278.879	2	7618.883	-2	7594.19	0	7606.385	0
41.5			3266.065	2	3278.560	2	7618.555	-1	7593.26	0	7605.755	-2
42.5			3265.430	0	3278.235	2	7618.216	4	7592.29	-21	7605.109	-4
43.5			3264.788	-1	3277.905	5	7617.839	-12	7591.36	3	7604.450	-3
44.5			3264.145	4	3277.568	7	7617.466	-8	7590.38	5	7603.774	-3
45.5			3263.488	1	3277.217	2	7617.081	0	7589.38	-8	7603.082	-2
46.5			3262.828	3	3276.867	5	7616.660	-12			7602.376	0
47.5			3262.150	-7	3276.510	7	7616.246	0	7587.35	-4	7601.650	-1
48.5			3261.464	-19	3276.138	1	7615.801	-2	7586.31	-6	7600.908	-2
49.5					3275.767	3			7585.27	9	7600.151	-1
50.5					3275.384	-2	7614.867	-1	7584.18	-4	7599.375	-3
51.5					3275.002	1	7614.378	3	7583.09	-1	7598.587	1
52.5			3258.720	0			7613.881	16	7581.98	-5	7597.779	1
53.5			3258.004	-9	3274.215	1	7613.339	2	7580.86	-8	7596.953	1
54.5			3257.303	2	3273.811	-1	7612.800	7	7579.73	9		
55.5			3256.589	5	3273.404	0	7612.230	-1	7578.58	10	7595.251	1
56.5			3255.860	0	3272.988	-3	7611.670	20	7577.39	4	7594.377	6
57.5			3255.127	-5	3272.565	-8	7611.060	8	7576.21	11	7593.483	6
58.5			3254.411	13	3272.142	-6	7610.441	5	7574.98	-2	7592.573	10
59.5			3253.652	-7	3271.712	-7	7609.822	20	7573.76	4	7591.632	1
60.5			3252.907	-7	3271.281	-6	7609.152	3			7590.689	7
61.5			3252.168	2	3270.836	-12	7608.490	13			7589.704	-9
62.5			3251.414	2	3270.406	-1	7607.783	-4			7588.721	-4
63.5			3250.648	-6	3269.969	9	7607.075	-1			7587.718	0
64.5					3269.509	-1	7606.334	-13			7586.687	-5
65.5					3269.065	9	7605.577	-21			7585.640	-7
66.5											7584.555	-27
67.5											7583.461	-37

	$C^4\Delta_{7/2}$ - $X^4\Phi_{9/2}$						$G^4\Phi_{9/2}$ - $C^4\Delta_{7/2}$					
	0 - 0						0 - 0					
J	R(J)	O-C	P(J)	O-C	Q(J)	O-C	R(J)	O-C	P(J)	O-C	Q(J)	O-C
6.5											7648.099	-2
7.5					3236.057	-8					7647.999	8
8.5			3233.300	3	3236.003	0	7650.742	-8			7647.871	5
9.5	3239.277	-1	3232.916	6	3235.934	-1	7650.906	-8			7647.727	1
10.5	3239.520	0	3232.503	-13	3235.854	-5	7651.056	-7			7647.571	1
11.5	3239.749	-6	3232.110	-4			7651.192	-4	7643.90	-8	7647.396	-4
12.5	3239.985	1	3231.709	3	3235.681	-5	7651.312	-3	7643.42	0	7647.223	7
13.5			3231.283	-7	3235.586	-2	7651.410	-8	7642.92	-3	7647.015	-2
14.5	3240.402	-15	3230.866	-1	3235.474	-9	7651.506	-1	7642.39	-9	7646.798	-5
15.5	3240.620	-3	3230.438	1	3235.367	-4	7651.582	0	7641.86	-10	7646.575	1

TABLE 1—*Continued*

	$C^4\Delta_{7/2}$ - $X^4\Phi_{9/2}$ 0 - 0						$C^4\Delta_{7/2}$ - $X^4\Phi_{9/2}$ 0 - 0					
J	R(J)	O-C	P(J)	O-C	Q(J)	O-C	R(J)	O-C	P(J)	O-C	Q(J)	O-C
16.5	3240.812	-10	3229.994	-5	3235.252	1	7651.639	-3			7646.331	0
17.5	3241.000	-13			3235.122	-3	7651.686	0	7640.77	5	7646.076	5
18.5	3241.189	-8	3229.099	-4	3234.985	-6	7651.716	1	7640.18	-7	7645.796	-2
19.5	3241.373	-1	3228.646	2	3234.850	0	7651.729	-1	7639.60	5	7645.508	-1
20.5	3241.537	-6	3228.174	-4	3234.705	4	7651.729	0	7638.99	0	7645.208	1
21.5	3241.709	3	3227.704	0	3234.550	5	7651.716	2	7638.37	2	7644.885	-3
22.5	3241.857	-3	3227.210	-13	3234.387	4	7651.686	2	7637.73	-3	7644.552	-3
23.5	3242.007	0	3226.736	0	3234.217	4	7651.639	0	7637.08	-1	7644.211	4
24.5	3242.150	3	3226.242	1	3234.041	6	7651.582	4	7636.42	6	7643.845	2
25.5			3225.741	4	3233.855	5	7651.506	4	7635.73	-2	7643.467	1
26.5	3242.412	7	3225.229	1	3233.662	4	7651.410	-2	7635.04	2	7643.075	2
27.5			3224.707	-4	3233.463	5	7651.312	6	7634.33	1	7642.665	0
28.5	3242.635	2	3224.188	1	3233.254	2	7651.192	6	7633.60	1	7642.244	2
29.5	3242.734	-3	3223.658	2	3233.040	3	7651.056	6	7632.86	1	7641.805	1
30.5	3242.829	-3	3223.118	0	3232.818	2	7650.906	7	7632.10	-1	7641.349	-1
31.5	3242.918	-2	3222.575	4	3232.590	2	7650.742	10	7631.33	-9	7640.882	0
32.5	3243.021	20	3222.021	3	3232.353	2	7650.559	8	7630.55	3	7640.404	5
33.5	3243.078	3	3221.464	6	3232.110	3	7650.358	4	7629.75	-1	7639.901	1
34.5	3243.172	32	3220.895	5	3231.858	1	7650.148	6	7628.94	8	7639.387	0
35.5	3243.219	20			3231.599	0	7649.921	6	7628.10	-2	7638.859	0
36.5	3243.264	14	3219.738	4	3231.334	0	7649.675	3	7627.25	-8	7638.314	-1
37.5	3243.302	9	3219.144	0	3231.059	-2	7649.415	1	7626.40	-1	7637.751	-4
38.5	3243.346	17	3218.551	4	3230.781	1	7649.141	0	7625.52	0	7637.180	-1
39.5	3243.392	34	3217.945	2	3230.495	3	7648.852	-1	7624.63	-1	7636.591	0
40.5			3217.327	-5	3230.199	2	7648.549	1	7623.72	-5	7635.987	0
41.5			3216.710	-3	3229.898	3	7648.229	0	7622.80	-9	7635.366	-1
42.5			3216.090	3	3229.580	-4	7647.887	-7	7621.86	-14	7634.730	-1
43.5			3215.453	-1	3229.269	2	7647.546	2	7620.90	-18	7634.077	-3
44.5			3214.811	-2	3228.943	1	7647.177	0	7619.95	-3	7633.414	-1
45.5			3214.166	1	3228.608	-2	7646.798	2	7618.97	0	7632.731	-2
46.5			3213.507	-3	3228.271	1	7646.396	-4	7617.97	0	7632.034	-2
47.5			3212.848	1	3227.923	0	7645.984	-4	7616.98	15	7631.326	2
48.5			3212.182	5	3227.569	1	7645.558	-2	7615.92	-9	7630.595	-2
49.5			3211.500	0	3227.210	4	7645.111	-5	7614.91	22	7629.850	-3
50.5			3210.815	-1	3226.837	1			7613.84	4	7629.094	-1
51.5			3210.123	0	3226.459	0	7644.186	3	7612.76	-4	7628.323	1
52.5			3209.426	2	3226.074	0	7643.691	-1	7611.67	-1	7627.528	-4
53.5			3208.716	0	3225.684	3	7643.181	-5	7610.57	-2	7626.726	-1
54.5			3208.002	-1	3225.282	1	7642.665	0	7609.45	5	7625.905	-3
55.5	3242.783	1	3207.287	7	3224.875	1	7642.131	3	7608.31	-3	7625.069	-3
56.5	3242.682	2			3224.464	5	7641.581	6	7607.16	0	7624.222	1
57.5			3205.815	0	3224.036	0	7641.009	2	7606.00	0	7623.353	-1
58.5	3242.456	2	3205.072	1	3223.606	0	7640.404	-19			7622.475	3
59.5			3204.323	3	3223.166	-2	7639.822	-1			7621.564	-11
60.5	3242.201	4	3203.550	-11	3222.725	3	7639.207	-1			7620.665	4
61.5	3242.055	-2	3202.798	5	3222.267	-2	7638.579	2			7619.731	-2
62.5	3241.915	6	3202.017	-3	3221.791	-17	7637.930	0			7618.790	2
63.5	3241.752	-1			3221.338	-2	7637.269	2			7617.839	11
64.5	3241.583	-7	3200.448	-1	3220.850	-13	7636.591	2			7616.842	-12
65.5			3199.647	-6	3220.373	-7	7635.899	4			7615.866	3
66.5	3241.231	-7	3198.855	6	3219.886	-2	7635.186	0			7614.867	10
67.5	3241.044	-7	3198.035	-2	3219.384	-4					7613.837	2
68.5	3240.857	2			3218.877	-4	7633.723	3			7612.800	2
69.5			3196.377	-14	3218.360	-5	7632.972	9			7611.753	7
70.5	3240.435	-5			3217.844	1					7610.692	14
71.5	3240.214	-6	3194.711	-4	3217.327	15	7631.407	3			7609.600	6
72.5			3193.868	3	3216.772	-1					7608.490	-5
73.5			3193.004	-4	3216.235	8					7607.386	4
74.5			3192.146	3	3215.671	-2					7606.252	0
75.5			3191.276	6	3215.113	2					7605.109	2
76.5			3190.394	4	3214.546	5					7603.948	1
77.5			3189.506	4	3213.970	6					7602.765	-6
78.5					3213.380	2					7601.577	-4
79.5											7600.366	-9
80.5											7599.132	-22

TABLE 2
Observed Line Positions (in cm^{-1}) for the $G^4\Phi - X^4\Phi$ Transition of TiCl

	$G^4\Phi_{3/2}$ - $X^4\Phi_{3/2}$											
	0 - 1				0 - 0				1 - 0			
J	R(J)	O-C	P(J)	O-C	R(J)	O-C	P(J)	O-C	R(J)	O-C	P(J)	O-C
2.5									11274.93	7		
3.5							10927.457	0	11275.14	5		
4.5							10927.055	0	11275.32	-2	11272.343	2
5.5							10926.622	-7	11275.48	-6	11271.910	2
6.5							10926.178	-3	11275.62	-6	11271.449	-1
7.5							10925.701	-9	11275.73	-9	11270.964	-4
8.5							10925.216	-1	11275.84	5	11270.461	0
9.5							10924.705	4			11269.935	5
10.5							10924.162	1			11269.376	0
11.5							10923.602	3			11268.797	1
12.5							10923.015	0	11275.95	-1	11268.190	-1
13.5							10922.408	1	11275.92	-2	11267.551	-12
14.5							10921.781	4	11275.85	-8	11266.910	0
15.5					10930.741	14*	10921.132	8	11275.78	-2	11266.234	2
16.5	10526.530	14*	10516.320	6	10930.666	16*	10920.447	-2	11275.67	0	11265.532	1
17.5	10526.487	41*			10930.585	33*	10919.763	13*	11275.55	0	11264.804	0
18.5	10526.437	83*	10514.971	18*	10930.520	90*	10919.044	15*	11275.39	1	11264.056	3
19.5	10526.203	-37*	10514.273	33*	10930.249	-37*	10918.318	32*	11275.21	0	11263.278	0
20.5	10526.086	-20*	10513.589	83*	10930.101	-17*	10917.617	99*	11275.01	2	11262.478	0
21.5	10525.945	-5	10512.720	-31*	10929.918	-10	10916.689	-41*	11274.78	2	11261.656	1
22.5	10525.770	-3	10511.960	-15*	10929.706	-9	10915.898	-19*	11274.53	0	11260.804	-2
23.5	10525.572	-3	10511.174	-4	10929.470	-9	10915.071	-11	11274.25	2	11259.934	1
24.5	10525.351	-3	10510.351	-9	10929.214	-6	10914.211	-14	11273.95	0	11259.035	-1
25.5	10525.111	-3	10509.520	1	10928.935	-3	10913.337	-7	11273.62	3	11258.116	3
26.5	10524.853	1	10508.661	2	10928.631	-3	10912.434	-7	11273.27	-1	11257.171	4
27.5	10524.566	-2	10507.775	-2	10928.302	-4	10911.511	-4	11272.90	2	11256.199	2
28.5	10524.263	0	10506.873	-1	10927.953	-2	10910.563	-3	11272.50	3	11255.203	1
29.5	10523.938	2	10505.946	-3	10927.580	-1	10909.593	-1	11272.07	-1	11254.184	1
30.5	10523.592	3	10505.006	2	10927.186	1	10908.600	0	11271.62	2	11253.139	0
31.5	10523.217	-3	10504.034	-3	10926.764	-2	10907.583	0	11271.15	2	11252.072	2
32.5	10522.832	3	10503.045	-4	10926.322	-1	10906.543	0	11270.65	0	11250.980	2
33.5	10522.417	0	10502.041	2	10925.858	0	10905.480	0	11270.13	4	11249.863	3
34.5	10521.988	4	10501.010	1	10925.368	-1	10904.398	4	11269.58	-1	11248.726	7
35.5	10521.534	4	10499.958	0	10924.862	4	10903.285	-1	11269.00	-3	11247.554	1
36.5	10521.053	-1	10498.894	9	10924.318	-6	10902.154	-1	11268.41	-3	11246.362	-1
37.5	10520.553	-2	10497.791	0	10923.764	-2	10900.997	-3	11267.79	-2	11245.150	1
38.5	10520.035	-2	10496.674	-1	10923.184	-2	10899.823	-1	11267.14	-5	11243.908	-2
39.5	10519.497	1	10495.535	-4	10922.582	0	10898.622	-2	11266.47	2	11242.640	-6
40.5	10518.933	-1	10494.376	-4	10921.955	-1	10897.402	0	11265.77	-5	11241.356	-2
41.5	10518.349	-2	10493.203	2	10921.315	9	10896.148	-8	11265.05	-3	11240.046	0
42.5	10517.747	1	10492.008	7	10920.635	2	10894.887	-1	11264.31	-2	11238.706	-3
43.5	10517.126	6	10490.782	3	10919.937	0	10893.608	11	11263.54	-2	11237.346	-2
44.5	10516.482	10	10489.538	2	10919.222	4	10892.280	-2	11262.75	1	11235.962	-1
45.5	10515.808	6	10488.257	-15	10918.476	0	10890.942	-3	11261.93	0	11234.552	-1
46.5	10515.113	2	10486.992	6	10917.712	1	10889.585	0	11261.09	1	11233.114	-5
47.5	10514.413	15	10485.678	-1	10916.900	-23	10888.204	1	11260.23	7	11231.651	-9
48.5	10513.665	1	10484.348	-2	10916.108	-3	10886.804	7	11259.34	13*	11230.186	9
49.5	10512.905	-3			10915.269	-7	10885.349	-20	11258.44	25*	11228.676	7
50.5	10512.130	0	10481.622	-8	10914.417	-1	10883.917	-1	11257.52	42*	11227.152	14*
51.5	10511.332	0	10480.234	-4	10913.548	11	10882.438	-5	11256.56	48*	11225.611	29*
52.5			10478.821	-3	10912.633	0	10880.942	-4			11224.041	40*
53.5	10509.667	-1	10477.388	-1	10911.707	2	10879.424	-1			11222.452	56*
54.5	10508.804	0	10475.928	-4	10910.757	3	10877.882	-1				
55.5	10507.914	-3	10474.453	-1	10909.779	-1						
56.5	10507.009	-1			10908.784	2	10874.725	-2				
57.5	10506.070	-11			10907.762	0	10873.118	4				
58.5	10505.132	2	10469.891	-1	10906.723	5	10871.484	4				
59.5	10504.154	-2					10869.821	-1				
60.5	10503.164	2	10466.742	0	10904.556	-4	10868.140	0				
61.5	10502.152	7	10465.133	-2	10903.441	-4	10866.435	-1				
62.5	10501.113	6	10463.502	-5	10902.309	2	10864.703	-5				
63.5	10500.044	-2	10461.856	-2	10901.157	10	10862.956	-2				
64.5	10498.969	4	10460.187	0	10899.957	-5	10861.189	4				
65.5			10458.492	-1	10898.757	3	10859.387	-1				
66.5	10496.740	5	10456.782	3	10897.523	0	10857.563	-5				

Note: O-C are observed minus calculated line positions in units of 10^{-3} cm^{-1} and asterisks mark perturbed lines.

TABLE 2—*Continued*

	$G^4\Phi_{3/2}$ - $X^4\Phi_{3/2}$											
	0 - 1				0 - 0				1 - 0			
J	R(J)	O-C	P(J)	O-C	R(J)	O-C	P(J)	O-C	R(J)	O-C	P(J)	O-C
67.5	10495.585	-2			10896.266	-2	10855.725	0				
68.5					10894.995	5	10853.857	-2				
69.5					10893.690	1	10851.968	-2				
70.5					10892.363	0	10850.049	-9				
71.5					10891.015	1	10848.125	2				
72.5					10889.640	-2	10846.164	0				
73.5					10888.253	7	10844.180	-2				
74.5					10886.842	16	10842.175	-2				
75.5							10840.150	1				
76.5							10838.096	-2				
77.5							10836.021	-2				
78.5							10833.924	-1				
79.5							10831.804	1				
80.5							10829.655	-4				
81.5							10827.487	-4				
82.5							10825.300	0				
83.5							10823.083	-1				
84.5							10820.850	3				
85.5							10818.588	3				
86.5							10816.304	4				
87.5							10813.995	3				

	$G^4\Phi_{5/2}$ - $X^4\Phi_{5/2}$											
	0 - 1				0 - 0				1 - 0			
J	R(J)	O-C	P(J)	O-C	R(J)	O-C	P(J)	O-C	R(J)	O-C	P(J)	O-C
4.5					10920.635	0						
5.5					10920.808	-1						
6.5					10920.963	3						
7.5					10921.080	-7					11259.853	-7
8.5	10516.926	3			10921.190	-2					11259.344	-6
9.5	10517.014	-5	10511.005	-1	10921.274	1	10915.269	11			11258.802	-14
10.5	10517.090	-4					10914.720	4			11258.258	1
11.5	10517.142	-5	10509.935	3			10914.156	6	11264.85	-3	11257.674	0
12.5	10517.185	6	10509.350	-13			10913.548	-12	11264.85	8	11257.069	3
13.5	10517.185	-5	10508.761	-11			10912.947	-1	11264.80	1	11256.436	4
14.5	10517.185	6	10508.151	-9			10912.305	-8	11264.74	-8	11255.783	9
15.5	10517.142	-3	10507.524	-3	10921.274	0	10911.652	-2	11264.66	-1	11255.091	-1
16.5	10517.090	-1	10506.873	1	10921.190	-3	10910.976	4	11264.54	-6	11254.386	1
17.5	10517.014	-1	10506.194	-1	10921.080	-8	10910.268	0	11264.41	-5	11253.654	1
18.5	10516.926	8	10505.493	-3	10920.963	2	10909.540	0	11264.25	-1	11252.898	2
19.5			10504.772	-5	10920.808	-2	10908.784	-5	11264.06	-15	11252.123	8
20.5	10516.656	-1	10504.034	-2	10920.635	-1	10908.012	-3	11263.87	6	11251.310	1
21.5	10516.482	-13	10503.264	-9	10920.447	8	10907.217	0	11263.64	10	11250.480	1
22.5	10516.318	8	10502.488	-1	10920.217	-1	10906.399	3	11263.37	1	11249.617	-6
23.5	10516.116	12	10501.681	-2	10919.977	2	10905.555	2	11263.07	-15	11248.726	-18
24.5	10515.881	5	10500.855	0	10919.707	-1	10904.692	6			11247.835	-4
25.5	10515.623	-3	10500.012	6	10919.420	3	10903.796	-1	11262.44	-11	11246.914	4
26.5	10515.360	5	10499.139	4	10919.102	-1	10902.880	-3	11262.09	-5	11245.952	-5
27.5	10515.057	-5	10498.257	14	10918.766	0	10901.946	0	11261.72	4	11244.975	-5
28.5	10514.744	-4	10497.330	1	10918.409	4	10900.997	10	11261.32	11	11243.973	-4
29.5	10514.413	2	10496.402	8	10918.023	1	10900.004	-1	11260.89	13	11242.930	-20
30.5	10514.070	18	10495.437	1	10917.618	4	10898.993	-5	11260.42	-2		
31.5	10513.665	-8	10494.460	3	10917.187	3	10897.971	2	11259.93	-5		
32.5	10513.295	25	10493.457	0	10916.735	6	10896.916	0	11259.44	5		
33.5	10512.847	1	10492.432	-2	10916.253	1	10895.842	2				
34.5	10512.403	2	10491.391	-1	10915.757	6	10894.745	3				
35.5	10511.956	23	10490.329	3	10915.230	3	10893.608	-11				
36.5	10511.455	10	10489.242	3	10914.678	-1	10892.475	2				
37.5	10510.932	-2	10488.128	-1	10914.107	-1	10891.305	0				
38.5	10510.417	17	10486.992	-7	10913.516	2	10890.116	3				
39.5	10509.840	-6	10485.854	6	10912.899	3	10888.899	1				

TABLE 2—*Continued*

	$G^4\Phi_{5/2}$ - $X^4\Phi_{5/2}$											
	0 - 1				0 - 0				1 - 0			
J	R(J)	O-C	P(J)	O-C	R(J)	O-C	P(J)	O-C	R(J)	O-C	P(J)	O-C
40.5	10509.267	-2	10484.675	1	10912.255	0	10887.658	-1				
41.5	10508.661	-10	10483.471	-7	10911.589	-1	10886.397	-1				
42.5	10508.054	4	10482.258	-3	10910.903	1	10885.113	0				
43.5	10507.403	-5	10481.028	5	10910.184	-6	10883.804	0				
44.5	10506.743	-2	10479.761	-1	10909.455	-1	10882.468	-6				
45.5	10506.070	11	10478.481	1	10908.692	-5	10881.113	-6				
46.5	10505.345	-7	10477.176	-1	10907.913	-3	10879.741	-1				
47.5	10504.620	-3	10475.854	2	10907.108	-3	10878.339	-1				
48.5	10503.868	-3	10474.506	1	10906.289	6	10876.913	-4				
49.5	10503.102	3			10905.428	-3	10875.476	6				
50.5	10502.310	6	10471.748	1	10904.556	-1	10873.998	-1				
51.5	10501.487	-2	10470.334	-3	10903.653	-6	10872.503	-4				
52.5	10500.666	15	10468.913	9	10902.735	-3	10870.990	0				
53.5	10499.780	-12	10467.455	5	10901.789	-5						
54.5	10498.894	-17	10465.972	-3	10900.824	-3	10867.890	0				
55.5	10498.012	3	10464.461	-16	10899.823	-13	10866.304	-1				
56.5	10497.087	1	10462.960	0	10898.817	-6	10864.703	5				
57.5	10496.149	8			10897.783	-4	10863.068	1				
58.5					10896.728	-1	10861.417	2				
59.5					10895.650	3	10859.741	2				
60.5					10894.545	2	10858.043	3				
61.5					10893.420	5	10856.313	-7				
62.5					10892.280	14	10854.580	3				
63.5					10891.106	11	10852.821	10				
64.5					10889.899	-1	10851.030	6				
65.5					10888.676	-8	10849.215	1				
66.5							10847.376	-6				
67.5							10845.526	-3				
68.5							10843.638	-15				
69.5							10841.723	-33				
70.5							10839.814	-24				

	$G^4\Phi_{7/2}$ - $X^4\Phi_{7/2}$											
	0 - 1				0 - 0				1 - 0			
J	R(J)	O-C	P(J)	O-C	R(J)	O-C	P(J)	O-C	R(J)	O-C	P(J)	O-C
6.5							10901.892	3				
7.5							10901.418	2			11246.699	-1
8.5							10900.920	-1			11246.181	-10
9.5							10900.405	2			11245.658	1
10.5			10495.637	-6			10899.861	-1			11245.096	-3
11.5			10495.098	0			10899.295	-4			11244.516	0
12.5			10494.528	-4			10898.712	0			11243.908	-2
13.5	10502.390	-7					10898.101	-2			11243.275	-3
14.5	10502.390	-2	10493.336	-1			10897.467	-4	11251.63	1		
15.5			10492.716	9	10906.485	9	10896.815	-2	11251.53	-11	11241.940	-2
16.5	10502.310	-8	10492.059	3	10906.399	-2	10896.148	9	11251.44	2	11241.239	3
17.5	10502.255	5	10491.391	6	10906.297	-8	10895.435	-5	11251.31	2	11240.512	5
18.5	10502.152	-8	10490.696	4	10906.183	-2	10894.712	-5	11251.16	2	11239.756	3
19.5	10502.041	-8	10489.980	2	10906.046	3	10893.970	-2	11250.98	4	11238.980	5
20.5	10501.922	5	10489.242	-1	10905.874	-4	10893.201	-2	11250.77	1	11238.177	5
21.5	10501.763	0					10892.412	0	11250.55	3	11237.346	1
22.5	10501.591	2	10487.713	3	10905.480	2	10891.598	-1	11250.30	4	11236.498	5
23.5	10501.396	3	10486.905	-6	10905.240	-4	10890.760	-2	11250.02	1	11235.610	-7
24.5	10501.180	4	10486.092	1			10889.899	-4	11249.72	3	11234.723	6
25.5	10500.943	6	10485.250	-1	10904.692	-15	10889.022	1	11249.39	5	11233.791	-1
26.5			10484.389	1	10904.398	-7	10888.119	3	11249.04	3	11232.846	4
27.5	10500.400	4	10483.516	11	10904.083	4	10887.195	5	11248.66	-2	11231.873	4
28.5	10500.097	4	10482.605	3	10903.738	7	10886.249	10	11248.26	-2	11230.876	5
29.5	10499.780	10	10481.678	2	10903.359	-1	10885.271	5	11247.84	-3	11229.846	-2
30.5	10499.424	-1	10480.722	-7	10902.968	2	10884.271	1	11247.39	-1	11228.792	-9
31.5	10499.060	1	10479.761	-1	10902.551	2	10883.251	-1	11246.91	-2	11227.722	-8

TABLE 2—*Continued*

	$G^4\Phi_{7/2}$ - $X^4\Phi_{7/2}$											
	0 - 1				0 - 0				1 - 0			
J	R(J)	O-C	P(J)	O-C	R(J)	O-C	P(J)	O-C	R(J)	O-C	P(J)	O-C
32.5	10498.665	-5	10478.772	-1	10902.110	2	10882.215	4	11246.42	-1	11226.636	2
33.5	10498.257	-5	10477.767	4			10881.146	-1	11245.89	-6	11225.513	-2
34.5	10497.837	6	10476.741	9	10901.157	-3	10880.058	-2	11245.35	-3	11224.363	-7
35.5	10497.382	3	10475.680	-1	10900.653	3	10878.949	-1	11244.78	0	11223.199	-3
36.5	10496.909	3	10474.605	-2	10900.120	1	10877.818	0	11244.18	-5	11222.006	-3
37.5	10496.402	-11	10473.503	-9	10899.563	0	10876.664	1	11243.56	0	11220.797	4
38.5	10495.892	-4			10898.993	8	10875.476	-9	11242.93	9	11219.545	-6
39.5	10495.360	1	10471.256	-3	10898.383	-1	10874.285	1	11242.27	21*	11218.290	5
40.5	10494.806	5	10470.090	-11	10897.757	-4	10873.062	0	11241.61	48*	11217.003	6
41.5	10494.216	-4	10468.913	-9	10897.112	-2	10871.814	-1	11240.96	114*	11215.705	23*
42.5	10493.621	2	10467.725	4	10896.440	-4	10870.545	-1			11214.393	49*
43.5	10492.991	-5	10466.494	-5	10895.747	-4	10869.253	-1			11213.091	109*
44.5	10492.352	0	10465.248	-8	10895.035	0	10867.943	4	11238.32	-222*		
45.5	10491.685	-2	10463.994	2	10894.296	0	10866.607	5	11237.54	-195*		
46.5	10490.996	-3	10462.705	-1	10893.532	-2	10865.240	-1	11236.72	-170*	11208.523	-228*
47.5	10490.282	-8	10461.395	-5	10892.746	-3	10863.860	1	11235.86	-170*	11207.107	-185*
48.5			10460.076	4	10891.938	-3	10862.451	-1	11234.97	-171*	11205.634	-176*
49.5	10488.814	6	10458.723	0	10891.106	-3	10861.022	-2	11234.05	-174*	11204.126	-177*
50.5	10488.042	8	10457.354	1	10890.252	-2	10859.570	-2	11233.11	-179*	11202.600	-173*
51.5	10487.242	2	10455.965	4	10889.376	-1	10858.096	-1	11232.14	-195*	11201.040	-177*
52.5	10486.436	12	10454.543	-5	10888.478	2	10856.597	-3	11231.15	-203*	11199.458	-181*
53.5	10485.581	-5	10453.119	6	10887.553	1	10855.077	-3	11230.13	-214*	11197.840	-195*
54.5	10484.729	3	10451.658	0	10886.617	13	10853.536	0	11229.08	-228*	11196.202	-207*
55.5	10483.854	9	10450.188	7	10885.624	-11	10851.968	-2	11228.01	-242*	11194.542	-216*
56.5	10482.965	23	10448.686	3	10884.643	1	10850.382	0	11226.90	-265*	11192.850	-234*
57.5	10482.011	-7	10447.160	-4	10883.626	1	10848.769	0	11225.78	-285*	11191.135	-251*
58.5	10481.081	9			10882.585	1	10847.135	0	11224.63	-308*	11189.393	-270*
59.5	10480.105	0			10881.518	-3	10845.476	-2	11223.46	-326*	11187.643	-274*
60.5	10479.132	17			10880.435	0	10843.796	-1	11222.25	-349*	11185.854	-293*
61.5	10478.097	-8			10879.337	12	10842.094	1	11221.03	-377*	11184.025	-328*
62.5					10878.191	-1	10840.366	-1	11219.77	-405*	11182.208	-328*
63.5	10476.020	3			10877.034	-3	10838.617	-1	11218.50	-429*	11180.322	-372*
64.5	10474.938	-4			10875.861	4			11217.19	-461*	11178.433	-396*
65.5	10473.841	-3							11215.87	-483*	11176.509	-431*
66.5									11214.51	-526*	11174.569	-459*
67.5												
68.5									11211.73	-590*	11170.607	-525*
69.5									11210.30	-622*	11168.593	-556*
70.5									11208.85	-659*	11166.552	-590*
71.5									11207.37	-697*	11164.495	-617*
72.5									11205.86	-740*	11162.399	-658*
73.5									11204.34	-773*	11160.285	-695*
74.5									11202.79	-814*	11158.148	-731*
75.5									11201.21	-860*	11155.977	-777*
76.5									11199.61	-899*	11153.792	-814*
77.5									11197.97	-951*	11151.580	-855*
78.5									11196.31	-1000*	11149.343	-898*
79.5									11194.64	-1044*	11147.072	-950*
80.5									11192.92	-1109*	11144.782	-999*
81.5											11142.483	-1033*
82.5											11140.136	-1092*
83.5											11137.774	-1143*
84.5											11135.373	-1210*
85.5											11132.963	-1263*
86.5											11130.535	-1310*
87.5											11128.073	-1369*
88.5												
89.5											11123.039	-1526*
90.5											11120.503	-1590*
91.5											11117.922	-1675*
92.5											11115.334	-1744*
93.5											11112.727	-1810*

TABLE 2—*Continued*

	$G^4\Phi_{9/2}$ - $X^4\Phi_{9/2}$											
	0 - 1				0 - 0				1 - 0			
J	R(J)	O-C	P(J)	O-C	R(J)	O-C	P(J)	O-C	R(J)	O-C	P(J)	O-C
2.5					10885.714	-9						
3.5					10885.942	-8	10883.505	-15				
4.5					10886.141	-13	10883.111	-7				
5.5					10886.323	-15	10882.688	-6				
6.5					10886.487	-11	10882.256	9			11228.429	1
7.5					10886.617	-19	10881.775	-3			11227.943	-2
8.5					10886.750	-4	10881.287	-2			11227.448	11
9.5					10886.842	-7	10880.776	0			11226.904	-1
10.5							10880.240	-1			11226.337	-12
11.5			10475.500	2	10886.970	-2	10879.687	2	11233.00	-3	11225.779	11
12.5			10474.938	-2	10887.003	3	10879.110	3	11233.00	-1	11225.162	-2
13.5	10482.859	-2	10474.357	-5			10878.513	6	11232.98	14	11224.525	-10
14.5	10482.859	-10	10473.764	1			10877.882	-2	11232.92	1	11223.882	1
15.5	10482.859	3			10886.937	-16	10877.241	1	11232.85	3	11223.199	-5
16.5	10482.821	-2			10886.898	5	10876.579	6	11232.75	1	11222.507	6
17.5	10482.768	-2	10471.841	-2	10886.804	-6	10875.893	8	11232.62	-1	11221.772	-4
18.5	10482.694	-1	10471.174	11	10886.710	3	10875.176	2	11232.47	-5	11221.026	0
19.5	10482.605	5	10470.464	2	10886.589	9	10874.444	3	11232.30	6	11220.237	-14
20.5	10482.481	-3	10469.735	-5	10886.434	3	10873.688	1	11232.10	-4	11219.444	-8
21.5	10482.346	-2	10468.994	-4			10872.916	6	11231.87	-7	11218.626	-2
22.5	10482.194	3			10886.069	2	10872.120	9	11231.65	18	11217.782	1
23.5	10482.011	-2	10467.455	2	10885.853	2	10871.293	3	11231.37	4	11216.904	-5
24.5	10481.816	1	10466.647	-2	10885.624	11	10870.448	1	11231.07	-1	11216.012	-1
25.5	10481.622	27	10465.829	4	10885.349	-3	10869.581	-1	11230.75	-1	11215.094	1
26.5	10481.353	-3	10464.976	-4	10885.068	-2	10868.697	3	11230.40	-6	11214.144	-3
27.5	10481.081	-14	10464.122	8	10884.770	5	10867.787	3	11230.04	2	11213.183	4
28.5	10480.818	5	10463.228	0	10884.439	2	10866.856	4	11229.64	2	11212.192	7
29.5	10480.515	3	10462.326	4	10884.091	3	10865.901	4	11229.22	1	11211.155	-13
30.5	10480.188	0	10461.395	1	10883.718	3	10864.924	3	11228.79	10	11210.125	-1
31.5	10479.848	4	10460.449	3	10883.319	-1	10863.922	0	11228.32	2	11209.061	2
32.5			10459.477	-1	10882.905	3	10862.902	1	11227.82	-2	11207.969	0
33.5	10479.089	-3	10458.492	4	10882.468	6	10861.858	1	11227.31	4	11206.854	1
34.5	10478.686	0	10457.483	5	10882.001	2	10860.788	-2	11226.77	0	11205.716	3
35.5	10478.257	-1	10456.447	1	10881.518	5	10859.699	-3	11226.21	4	11204.547	-3
36.5	10477.810	2	10455.387	-8	10881.007	1	10858.597	6	11225.61	-4	11203.363	2
37.5	10477.334	-4	10454.322	0	10880.480	5	10857.459	1	11225.00	1	11202.148	0
38.5	10476.846	-1	10453.233	5	10879.918	-3	10856.313	10	11224.36	1	11200.916	5
39.5	10476.330	-4			10879.337	-7	10855.127	3	11223.70	-1	11199.654	4
40.5	10475.799	-2	10450.977	-1	10878.750	5	10853.921	-2	11223.01	0	11198.362	-2
41.5	10475.250	4	10449.817	-5	10878.124	1	10852.695	-4	11222.30	3	11197.058	5
42.5	10474.671	1	10448.646	2	10877.474	-4	10851.452	-2	11221.56	3	11195.720	2
43.5	10474.073	1	10447.441	-5	10876.806	-5	10850.190	5	11220.80	-2	11194.364	5
44.5	10473.459	6	10446.229	3	10876.113	-7	10848.893	0	11220.02	4	11192.977	1
45.5			10444.995	9	10875.407	1	10847.581	1	11219.20	-1	11191.570	3
46.5			10443.731	6	10874.670	0	10846.245	2	11218.36	1	11190.139	4
47.5	10471.472	3	10442.440	-3	10873.906	-4	10844.878	-6	11217.50	0	11188.676	-1
48.5	10470.754	-11	10441.133	-6	10873.118	-9	10843.502	1			11187.194	-2
49.5			10439.811	-3	10872.320	-2	10842.094	-3	11215.71	-1	11185.690	1
50.5	10469.297	5	10438.468	0	10871.484	-9	10840.669	0	11214.78	5	11184.166	8
51.5	10468.525	1	10437.105	4	10870.639	-2	10839.218	-1	11213.82	13	11182.608	5
52.5	10467.725	-8	10435.715	3	10869.767	1	10837.745	0	11212.81	-10	11181.026	3
53.5	10466.912	-10	10434.291	-11	10868.869	0	10836.247	-2	11211.81	-4	11179.417	-1
54.5	10466.076	-12	10432.873	1	10867.943	-4	10834.728	-2	11210.79	6	11177.790	2
55.5	10465.248	15	10431.421	2	10866.998	-4	10833.183	-5	11209.72	-4	11176.137	2
56.5					10866.032	-3	10831.617	-6	11208.65	18	11174.450	-6
57.5	10463.450	-8	10428.455	5	10865.041	-2	10830.033	-3	11207.53	2		
58.5	10462.559	21	10426.933	-2	10864.028	-1	10828.423	-2	11206.39	1	11171.026	1
59.5	10461.599	2	10425.397	0	10862.994	3	10826.789	-3	11205.23	-4		
60.5	10460.641	8	10423.836	-2	10861.932	2	10825.133	-2	11204.04	0	11167.499	4
61.5	10459.652	3			10860.844	-2	10823.452	-3	11202.84	2	11165.689	-4

TABLE 2—*Continued*

	$G^4\Phi_{9/2}$ - $X^4\Phi_{9/2}$											
	0 - 1				0 - 0				1 - 0			
J	R(J)	O-C	P(J)	O-C	R(J)	O-C	P(J)	O-C	R(J)	O-C	P(J)	O-C
62.5	10458.633	-8			10859.741	3	10821.748	-5	11201.60	0	11163.863	-3
63.5	10457.618	5					10820.025	-2	11200.34	-1	11162.017	2
64.5	10456.521	-42					10818.275	-3	11199.05	-6	11160.127	-12
65.5	10455.491	0			10856.276	1	10816.511	4	11197.74	-2	11158.240	3
66.5	10454.398	1			10855.077	3	10814.709	-3	11196.41	4	11156.314	3
67.5	10453.289	8			10853.857	9	10812.897	3	11195.04	0	11154.364	3
68.5					10852.605	4	10811.051	-2			11152.388	3
69.5					10851.329	0	10809.187	-2	11192.25	5	11150.376	-8
70.5					10850.049	15	10807.298	-4	11190.81	-2	11148.355	-4
71.5					10848.718	2	10805.391	-2			11146.309	0
72.5					10847.376	2	10803.464	5	11187.86	-1	11144.229	-4
73.5					10846.017	7	10801.506	2	11186.34	0	11142.132	-1
74.5					10844.623	2					11140.003	-5
75.5					10843.209	0					11137.858	0
76.5					10841.765	-10					11135.683	1
77.5					10840.312	-3					11133.478	-4
78.5					10838.837	3					11131.250	-7
79.5					10837.325	-4					11129.001	-5
80.5					10835.801	1					11126.722	-8
81.5											11124.436	7
82.5											11122.103	-1
83.5											11119.765	12
84.5											11117.386	9
85.5											11114.986	11
86.5											11112.547	-1
87.5											11110.102	7
88.5											11107.609	-9

TABLE 3

Molecular Constants (in cm^{-1}) for the $X\,^4\Phi$ State of TiCl

	$X^4\Phi_{3/2}$		$X^4\Phi_{5/2}$	
Const.[a]	v=0	v=1	v=0	v=1
T_{vv}	0.0	404.3663(22)	0.0	404.3337(15)
B_v	0.1614799(55)	0.1606776(60)	0.1619046(79)	0.1610994(81)
$10^7 \times D_v$	1.0279(76)	1.0160(90)	0.978(15)	0.959(17)
	$X^4\Phi_{7/2}$		$X^4\Phi_{9/2}$	
Const.	v=0	v=1	v=0	v=1
T_{vv}	0.0	404.3167(14)	0.0	404.3032(13)
B_v	0.1623570(66)	0.1615485(69)	0.1628287(48)	0.1620202(50)
$10^7 \times D_v$	1.029(13)	1.021(15)	1.0699(66)	1.0688(77)

[a]The numbers in parentheses are one standard deviation in last two digits.

TABLE 4
Molecular Constants (in cm^{-1}) for the $C^4\Delta$ State of TiCl

	$C^4\Delta_{1/2}$	$C^4\Delta_{3/2}$	$C^4\Delta_{5/2}$	$C^4\Delta_{7/2}$
Const.[a]	v=0	v=0	v=0	v=0
T_{vv}	3363.48723(59)	3326.1079(29)	3285.41554(77)	3236.29528(58)
B_v	0.1565989(55)	0.157621(27)	0.1584356(68)	0.1592168(48)
$10^7 \times D_v$	0.9798(77)	2.09(65)	0.972(17)	1.1667(67)
$10^{10} \times H_v$	--	2.46(48)	0.0740(18)	--

[a]The numbers in parentheses are one standard deviation in last two digits.

shown in this figure, the lowest a^4F term of Ti^+, arising from the $3d^24s^1$ configuration (*37*), correlates to the $X^4\Phi$, $A^4\Sigma^-$, $B^4\Pi$, and $C^4\Delta$ states in TiCl, TiF, and TiH. The first excited energy term of Ti^+ is b^4F at $\sim$1000 cm^{-1}. This term arises from the $3d^3$ configuration (*37*) and correlates to the next set of four states $^4\Sigma^-$, $^4\Delta$, $^4\Phi$, and $^4\Pi$ for TiCl, TiF, and TiH. The third Ti^+ term, a^2F ($3d^24s^1$) at 4700 cm^{-1}, correlates with the $a^2\Delta$, $b^2\Pi$, $c^2\Phi$, and $d^2\Sigma^-$ states of the diatomics. The doublet states of TiCl and TiF have not been drawn in Fig. 1 to avoid complexity. It seems that the general picture of the low-lying states of TiCl, TiF, and TiH can be qualitatively predicted easily from the energy levels of Ti^+. Further calculations and experiments are necessary to verify these correlations. Although we have no proof that the ground state of TiCl is $X^4\Phi$, this assignment seems very likely.

In a simple ionic bonding model for TiCl one of the four valence electrons of the Ti atom is transferred to Cl and there

TABLE 5
Molecular Constants (in cm^{-1}) for the $G^4\Phi$ State of TiCl

	$G^4\Phi_{3/2}$		$G^4\Phi_{5/2}$	
Const.[a]	v=0	v=1	v=0	v=1
T_{vv}	10928.68724(71)	11273.9866(11)	10919.2666(10)	11262.8920(22)
B_v	0.1500983(56)	0.1492453(60)	0.1503661(82)	0.149519(12)
$10^7 \times D_v$	1.1268(79)	1.042(13)	1.288(20)	0.802(83)
$10^{10} \times H_v$	--	--	0.0460(21)	--
	$G^4\Phi_{7/2}$		$G^4\Phi_{9/2}$	
Const.	v=0	v=1	v=0	v=1
T_{vv}	10904.40590(73)	11249.7333(17)	10884.75612(69)	11230.97849(77)
B_v	0.1509790(65)	0.1500739(80)	0.1518472(49)	0.1506907(49)
$10^7 \times D_v$	1.104(13)	0.887(32)	1.5085(82)	1.2105(70)
$10^{10} \times H_v$	--	--	0.01824(47)	--

[a]The numbers in parentheses are one standard deviation in last two digits.

are three remaining electrons in metal-centered orbitals. The $X\,^4\Phi$ state of TiCl arises from the $\sigma^1\pi^1\delta^1$ configuration and the low-lying $A^4\Sigma^-$, $B^4\Pi$, and $C^4\Delta$ states arise from the $\sigma^1\delta^2$, $\pi\delta^2$, and $\pi^2\delta^1$ configurations, respectively.

The constants of Table 3 indicate that the $\Delta G(1/2)$ values of the individual spin components of TiCl ground state [$X\,^4\Phi_{3/2}$ (404.3663 cm^{-1}), $X\,^4\Phi_{5/2}$ (404.3337 cm^{-1}), $X\,^4\Phi_{7/2}$ (404.3167 cm^{-1}), and $X\,^4\Phi_{9/2}$ (404.3032 cm^{-1})] are very similar, consistent with an unperturbed, relatively isolated $X\,^4\Phi$ state. The $\Delta G(1/2)$ values of the $G^4\Phi$ state [$G^4\Phi_{3/2}$ (345.2994 cm^{-1}), $G^4\Phi_{5/2}$ (343.6254 cm^{-1}), $G^4\Phi_{7/2}$ (345.3274 cm^{-1}), and $G^4\Phi_{9/2}$ (346.2224 cm^{-1})] (Table 5) show more variation pointing to global interactions with other states. The $\Delta G(1/2)$ values of the $C^4\Delta$ state could not be determined because of the weak intensity of bands involving $v > 0$. The observed local perturbations in the $C^4\Delta$ state also indicate the presence of a close-lying electronic state (or states) interacting with the $C^4\Delta$ state. The $B^4\Pi$ state is the most suitable candidate, although interactions with other low-lying doublet and quartet states cannot be ruled out.

In the absence of cross transitions that determine the spin–orbit intervals, we have chosen to use a simple empirical term energy expression (Eq. [1]) to evaluate the effective molecular constants for the different spin components (Tables 3–5). The determination of the Hund's case (a) constants from the effective constants proceeded using the equations for a $^4\Phi$ state (*27*) and for a $^4\Delta$ state (*35*). The Hund's case (a) rotational constants for the $X\,^4\Phi$ state obtained in this way are $B''_0 = 0.16214$ cm^{-1}, $B''_1 = 0.16134$ cm^{-1}, and $A''_0 = 39$ cm^{-1}. The spin–orbit splitting constant of $A''_0 = 39$ cm^{-1} for TiCl is in good agreement with a value of 35 cm^{-1} obtained for TiF (*27*). The rotational constants for the ground state result in the equilibrium constants of $B''_e = 0.16254$ cm^{-1}, $\alpha''_e = 0.00080$ cm^{-1}, and $r''_e = 2.2647$ Å. In a similar fashion the constants $B_0 = 0.15797$ cm^{-1} and $A_0 = 29$ cm^{-1} for the $C^4\Delta$ state and $B_0 = 0.15082$ cm^{-1}, $B_1 = 0.14988$ cm^{-1}, and $A_0 = 26$ cm^{-1} for the $G^4\Phi$ state have been obtained. The constants of the $G^4\Phi$ state give $B_e = 0.15129$ cm^{-1}, $\alpha_e = 0.00094$ cm^{-1}, and $r_e = 2.3474$ Å. By averaging, the $\Delta G(1/2)$ values 404.33 and 345.12 cm^{-1} have been obtained for the $X\,^4\Phi$ and $G^4\Phi$ states, respectively.

CONCLUSIONS

In conclusion, the emission spectrum of TiCl in the 3000–12 000 cm^{-1} region has been investigated at high resolution using a Fourier transform spectrometer. The three groups of prominent bands in this region have been assigned as $C^4\Delta$–$X\,^4\Phi$, $G^4\Phi$–$X\,^4\Phi$, and $G^4\Phi$–$C^4\Delta$ transitions. A rotational analysis of these bands has been made and the molecular constants have been determined. The lowest $^4\Phi$ state has been tentatively assigned as the ground state of TiCl consistent with our recent experimental observations of TiF (*27*) and theoretical predictions of Harrison (*28*) for TiF. The ground state of TiCl is a well-behaved Hund's case (a) $^4\Phi$ state with $\Delta G(1/2) = 404.33$ cm^{-1} and $r_e = 2.2647$ Å.

ACKNOWLEDGMENTS

We thank J. Wagner, C. Plymate, and M. Dulick of the National Solar Observatory for assistance in obtaining the spectra. The National Solar Observatory is operated by the Association of Universities for Research in Astronomy, Inc., under contract with the National Science Foundation. The research described here was supported by funding from NASA laboratory astrophysics program. Some support was also provided by the Petroleum Research Fund administered by the American Chemical Society and the Natural Sciences and Engineering Research Council of Canada.

REFERENCES

1. C. Jascheck and M. Jascheck, ''The Behaviour of Chemical Elements in Stars.'' Cambridge Univ. Press, Cambridge, UK, 1995.
2. P. W. Merrill, A. J. Deutsch and P. C. Keenan, *Astrophys. J.* **136,** 21–34 (1962).
3. H. Machara and Y. Y. Yamashito, *Publ. Astron. Soc. Jpn.* **28,** 135–140 (1976).
4. R. S. Ram, P. F. Bernath, and L. Wallace, *Astrophys. J. Suppl. Ser.* **107,** 443–449 (1996).
5. A. J. Sauval, *Astron. Astrophys.* **62,** 295–298 (1978).
6. S. Wyckoff and R. E. S. Clegg, *Mon. Not. R. Astron. Soc.* **184,** 127–143 (1978).
7. N. M. White and R. F. Wing, *Astrophys. J.* **222,** 209–219 (1978).
8. D. L. Lambert and R. E. S. Clegg, *Mon. Not. R. Astron. Soc.* **191,** 367–389 (1978).
9. R. Yerle, *Astron. Astrophys.* **73,** 346–353 (1979).
10. B. Lindgren and G. Olofsson, *Astron. Astrophys.* **84,** 300–303 (1980).
11. P. K. Carroll, P. McCormack, and S. O'Connor, *Astrophys. J.* **208,** 903–913 (1976).
12. D. L. Lambert and E. A. Mallia, *Mon. Not. R. Astron. Soc.* **151,** 437–447 (1971).
13. O. Engvold, H. Wöhl, and J. W. Brault, *Astron. Astrophys. J. Suppl.* **42,** 209–213 (1980).
14. J. Cernicharo and M. Guélin, *Astron. Astrophys.* **183,** L10–L12 (1987).
15. L. M. Ziurys, A. J. Apponi, and T. G. Phillips, *Astrophys. J.* **433,** 729–732 (1994).
16. M. D. Allen and L. M. Ziurys, *J. Chem. Phys.* **106,** 3494–3503 (1997).
17. M. Tanimoto, S. Saito, and T. Okabayashi, *Chem. Phys. Lett.* **242,** 153–156 (1995).
18. A. Fowler, *Proc. R. Soc. London A* **79,** 509 (1907).
19. K. R. More and A. H. Parker, *Phys. Rev.* **52,** 1150–1152 (1937).
20. V. R. Rao, *Ind. J. Phys.* **23,** 535 (1949).
21. E. A. Shenyavskaya, Y. Y. Kuzyakov, and V. M. Tatevskii, *Opt. Spectrosc.* **12,** 197–199 (1962).
22. A. Chatalic, P. Deschamps and G. Pannetier, *C. R. Acad. Sci. Paris* **268,** 1111–1113 (1969).
23. R. L. Diebner and J. G. Kay, *J. Chem. Phys.* **51,** 3547–3554 (1969).
24. K. P. Lanini, Ph.D. dissertation, University of Michigan, Ann Arbor, Michigan, 1972.
25. T. C. DeVore, *High Temp. Sci.* **15,** 263–273 (1982).
26. J. G. Phillips and S. P. Davis, *Astrophys. J. Suppl. Ser.* **71,** 163–172 (1989).

27. R. S. Ram, J. R. D. Peers, Y. Teng, A. G. Adam, A. Muntianu, P. F. Bernath, and S. P. Davis, *J. Mol. Spectrosc.,* in press.
28. J. F. Harrison, private communication.
29. J. Anglada, P. J. Bruna, and S. D. Peyerimhoff, *Mol. Phys.* **69,** 281–303 (1990).
30. A. G. Gaydon, *J. Phys. B.* **7,** 2429–2432 (1974).
31. T. C. Steimle, J. E. Shirley, B. Simard, M. Vasseur, and P. Hackett, *J. Chem. Phys.* **95,** 7179–7182 (1991).
32. O. Launila and B. Lindgren, *J. Chem. Phys.* **104,** 6418–6422 (1996).
33. R. B. Le Blanc, J. B. White, and P. F. Bernath, *J. Mol. Spectrosc.* **164,** 574–579 (1994).
34. R. S. Ram, P. F. Bernath, and S. P. Davis, *J. Chem. Phys.* **104,** 6949–6955 (1996).
35. R. S. Ram, P. F. Bernath, and S. P. Davis, *J. Mol. Spectrosc.* **179,** 282–298 (1996).
36. R. S. Ram and P. F. Bernath, *J. Mol. Spectrosc.,* **183,** 263–272 (1997).
37. C. E. Moore, ‘‘Atomic Energy Levels,’’ Vol. I. Natl. Bur. of Standards, Washington, DC, 1949.